Mud in sandy riverbed deposits as a proxy for ancient fine-

2 sediment supply

- 3 N. Wysocki¹ and E. Hajek¹
- ¹Department of Geosciences, Penn State University, 534 Deike Building, University Park, PA
- 5 16802

6 ABSTRACT

7 The amount of silt and clay available to rivers reflects source-terrain composition and weathering 8 and can be a primary control on the form and dynamics of channel networks. Fine sediment also 9 affects the permeability of buried fluvial reservoirs. Despite this significance, we currently lack 10 methods for reconstructing how much fine sediment was transported by ancient rivers. Mud 11 accumulations in sandy river deposits are often interpreted as indicators of variable flow 12 conditions; however, these deposits may present an opportunity to constrain how much fine 13 sediment was transported through ancient rivers. Here we report results from a series of 14 experiments designed to evaluate how much clay and silt are preserved in sandy riverbed deposits 15 under constant and variable discharge conditions. Our results demonstrate that 1) mud deposits, 16 including drapes and lenses, form readily under constant, high-discharge conditions, 2) the amount 17 of fine sediment recovered from bed-material deposits increases as fine-sediment supply increases, 18 and 3) fine-sediment retention is higher during bed aggradation than during bypass conditions. 19 These results indicate that the net retention of clay and silt in sandy riverbed deposits may be a 20 simple but powerful proxy for comparing the overall amount of fine sediment supplied to ancient 21 rivers.

22 INTRODUCTION

The amount of fine sediment (silt and clay) in sand-bed rivers significantly influences channel form and movement and the architecture of fluvial deposits at a wide range of scales (e.g., Peakall et al., 2007; Hampson et al., 2014; Ghinassi et al., 2016; Lapôtre et al., 2019; Dunne and Jerolmack, 2020). Our ability to interpret the sedimentary archive of fluvial landscape dynamics and predict subsurface reservoir and aquifer quality is currently limited by a lack of constraints on fine-sediment flux to ancient rivers. Estimates of paleo-fine-sediment supply would help resolve outstanding questions about, for example, controls on river form and mobility in Earth's past (e.g., Davies and Gibling, 2011; McMahon and Davies, 2018; Ganti et al., 2019), or how climate-mediated changes in sediment supply, water discharge, or land cover are recorded in fluvial strata (e.g., Foreman et al., 2012; Foreman, 2014; Colombera et al., 2017).

Mechanisms for mud deposition in alluvial channels are varied and still being explored. Based strictly on particle size, silt and clay have slow settling velocities; consequently, mud deposits in sand-bed channels are commonly attributed to periods of slow or stagnant flow (e.g., Martin, 2000). In contrast, significant mud transport and deposition can occur during high-energy, high-concentration flows, which can be common in tidal or highly seasonal channels (e.g., Dalrymple and Choi, 2007; Plink-Björklund, 2015). Flocculation and mud aggregates allow silt and clay to behave like larger particles and interact with the channel bed (e.g., Rust and Nanson, 1989; Lamb et al., 2020), and advective pumping through bedforms can inject fine sediment into bed material (Packman and MacKay, 2003). Large channel-bed features like bars also create locally variable flow conditions which can promote suspended-sediment deposition (e.g., Szupiany et al., 2012) and enhance bed-deposit preservation (Ganti et al., 2020).

The role these mud transport and deposition processes play in controlling channel kinematics, floodplain aggradation, and sediment mass balance in fluvial systems remains

unconstrained. Consequently, it is difficult to uniquely interpret the factors that controlled mud accumulation in ancient fluvial deposits. Conceptually, rivers fed by muddy source areas should carry and deposit a larger proportion of fine-sediment than those with mud-poor sources. To test this principle, we conducted a series of experiments to evaluate whether the amount of fine sediment supplied to sandy rivers could be reflected in the amount of mud retained in their deposits. Our experiments were designed to constrain the amount and character of fine-sediment deposits that accumulate under constant, high flow conditions and provide insight into how mud deposited with channel-bed material might record overall fine-sediment flux or flow intermittency in ancient systems.

EXPERIMENTAL DESIGN

A series of five flume experiments were conducted at the St. Anthony Falls Laboratory (Figure 1; details in Supplement). Water and sediment discharge were set to aggrade a sand bed via a wedge of sediment that prograded down the flume during each run; this is analogous to a bar with superposed bedforms migrating downstream in a river. Total water discharge for each run was 21 l/s (sufficient to transport sand as suspended load; e.g., Wilkerson and Parker, 2011) and was monitored an acoustic Doppler velocimeter (ADV) and by measuring the water depth over the weir at the end of the flume. Sand (median grainsize D_{50} =0.343 mm) and kaolin clay (D_{50} =0.004 mm) were supplied to the flume at a constant rate during each run (15 g/s sand and various clay concentrations; Table). Weir height was fixed, allowing the bed to aggrade ~6 cm in about four hours and each run was continued at bypass (i.e. no net bed aggradation) for 15-30 minutes.

Four runs had constant water discharge and one had intermittent water discharge (Table). The four constant discharge runs had clay concentrations of 0.0, 1000, 4000, 8500 mg/l. The intermittent-discharge experiment had low clay concentration (1000 mg/l) and every hour water

and sediment discharge were stopped, allowing fine sediment to settle onto the bed for >1 hr during each pause. All runs were equivalent to the fully turbulent flows of Baas et al. (2016; details in Supplement). Each run was recorded from the side of the flume with a video camera and photographs. These images were used to reconstruct bed topography and measure bed aggradation, bedform scale, and bedform migration rates in each run.

Fine-sediment mapping and sampling mimicked what could be accomplished in an outcrop. Fine-sediment accumulations were mapped on photographs of the flume wall (analogous to mapping an outcrop photo panel; Figure 2). After each experiment the bed was dried for two days, excavated, and sampled (analogous to collecting a hand-sample of ancient bed material from an outcrop). Samples were collected from bed deposits that accumulated during the aggradational and bypass phases of the experiment and were wet-sieved to determine the fraction of fine sediment.

RESULTS

Fine-sediment accumulations in experimental bed deposits included lenses, drapes, and interstitial fines (Figure 2; Table). Visible mud accumulations were most prominent in deposits from the high-concentration run, with most of the bed showing intersitial fines along with numerous bedform-scale lenses and continuous drapes of fine sediment. Interstitial fines were less noticeable in the intermediate-discharge run, but bed deposits contained mud lenses and some continuous mud drapes. Bed deposits from the low-concentration run contained some fine-sediment drapes. Deposits from the intermittent run contained discontinuous drapes.

The proportion of fines in bed-material deposits increased with higher fine-sediment concentrations (Table). For all but the low-concentration constant-discharge run, the average weight percent of fine sediment in a given sample significantly exceeded what would be expected

if fine-sediment retention were only due to interstitial fines in the bed (i.e. fine-sediment concentration x bed pore volume). Additionally, the highest fine-sediment retention occurred during aggradational phase of each run (Table). Bed-deposit samples from the intermittent-discharge run showed higher mud retention than the constant-discharge run with the same fine-sediment concentration.

DISCUSSION

Experiments with constant, high-discharge conditions produced deposits similar to those typically considered diagnostic of variable flow (e.g., mud drapes and flaser-like bedding; e.g., Boggs, 2012). This highlights that the presence of drapes and lenses in channel deposits does not uniquely indicate discharge intermittency in ancient rivers. The intermittent-discharge experiment retained more mud than its constant-discharge counterpart, suggesting that flow variability may enhance fine sediment deposition to some degree even in low-concentration flows. However, results of these experiments indicate that the overall flux of mud through a system may be the dominant control on the amount of fine sediment deposited in sandy riverbeds.

Mud deposits were most prevalent on the lee sides of individual bedforms (e.g., Figure 2). This pattern contrasts with other experiments where fine sediment accumulated in the bed on the upstream side of dunes through advective pumping and hyporheic exchange (Packman and MacKay, 2003) and is consistent with examples of systems with mud flocs and aggregates that hydrodynamically behave like coarser (e.g., sand-sized) particles (e.g., Rust and Nanson, 1989; Schieber et al., 2007; Matsubara et al., 2015; Mooneyham and Strom, 2018). The degree to which mud aggregates facilitated fine-sediment deposition in these experiments is unresolved; some sand-sized mud aggregates were seen along the glass wall of the flume near the bed of the experiments confirming their presence in the flume, and overall retention of clay in the bed is

consistent with that reported in the data compilation of de Leeuw et al. (2020) and Lamb et al. (2020) (Supplement). However, measured suspended-sediment concentrations were constant with depth, a pattern more characteristic of wash-load rather than suspended-load floc transport (Lamb et al., 2020). The presence of flocs in these experiments underscores the potential importance of flocculation in systems not generally considered strongly prone to floc formation (e.g., freshwater settings or rivers with modest clay concentrations), but further investigations will be necessary to determine whether flocs or aggregates drive the deposition of muddy lenses, drapes, and interstitial fines in sandy riverbed deposits.

115

116

117

118

119

120

121

122

123

124

125

126

127

128

129

130

131

132

133

134

135

136

137

Mud accumulations were most prevalent among bedforms deposited during the aggradational phase of the experiments downstream of the sediment wedge. This result is consistent with field data showing silt and clay accumulations in channel beds downstream of bars in modern rivers and ancient deposits (e.g., Lynds and Hajek, 2006; Hajek et al., 2010). The prograding sediment wedge may have enhanced fine-sediment accumulations during the aggradational phase by locally sequestering sand and decreasing the effective sand flux (thereby increasing the relative fines flux) downstream of the wedge. A lower relative sand flux is reflected by observed bedform-migration rates that were ~8 times slower during the aggradation phase (1.1-1.8 cm/s) than the bypass phase (8.6-12.0 cm/s) even though total supplied sediment flux was constant. This slower migration rate could have permitted more fine sediment to settle in the recirculation zone downstream of bedforms (Supplement). Preservation during the aggradational phase of the experiments was likely enhanced by an abrupt increase in local aggradation as the sediment wedge passed through the flume. In these experiments and field-scale systems, bar migration can rapidly bury slower-moving bedforms, thereby preserving them entirely (e.g., well preserved cross sets in Figure 2; Reesink et al., 2015; Ganti et al., 2020).

Overall, when more fine sediment was added to the flume, more fine-sediment was incorporated into bed deposits, suggesting that the bulk fraction of fine sediment preserved in ancient bed-material deposits may reflect the amount of fine sediment supplied to an ancient river. While progress has been made quantifying paleo-bedload transport in ancient rivers (e.g., Brewer et al., 2020), it remains difficult to reconstruct the fine-sediment flux. The possibility of comparing, even in a relative sense, the proportion of fine sediment moving through ancient rivers provides an important opportunity to attempt complete mass-balance estimates for ancient source-to-sink systems and understand controls on fine-sediment storage and bypass in sedimentary basins (e.g., Chamberlin and Hajek, 2019).

More work is needed to determine how to quantify fine-sediment flux from ancient fluvial deposits and to understand the relative contributions of flow intermittency, flocculation, and other processes that drive mud deposition. However, in the near term, these results indicate that the amount of mud preserved in bed-material deposits (e.g., cross sets from channel sandstones) may provide a benchmark for normalizing and comparing fine-sediment storage at larger scales. Bed-material samples from channel sandbodies spanning documented alluvial architecture transitions could help determine whether and how the fraction of fine sediment in ancient rivers changed along with trends in, for example, channel-body dimensions, floodplain facies, and the overall proportion of channel sediments preserved at different places and times within a basin (e.g., Foreman, 2014; Hampson, 2016; Chamberlin and Hajek, 2019; Wang and Plink-Björklund, 2019).

Relative comparisons of paleo-fine-sediment flux may help answer outstanding questions about changes in hillslope weathering or the role of cohesive sediment in controlling river dynamics through Earth's history (e.g., Foreman et al., 2012; Ielpi and Lapôtre, 2020). Furthermore, constraining the fraction of fines present in bed-material deposits will be helpful for

more accurately predicting heterogeneity and compartmentalization in fluvial reservoirs. Measuring the fraction of fines in ancient bed-material deposits offers a tractable, potentially powerful approach to reconstructing and comparing paleo-fine-sediment loads through Earth's history.

CONCLUSIONS

These experiments demonstrate that the proportion of fine sediment trapped in sandy riverbed material can reflect the concentration of clay and silt available in the flow. While discharge intermittency may enhance mud deposition for a given fine-sediment flux, our results show that the amount of mud hosted in riverbed deposits may primarily reflect the total supplied fine-sediment load rather than variable discharge. These results highlight a need for more targeted studies aimed at constraining the role of flocculation and local sorting in mixed sand-mud systems and improving our understanding of how interactions of bedforms and larger features like bars influence fine-sediment deposition and preservation in ancient deposits. Measuring mud fractions preserved in riverbed deposits can provide an important avenue for reconstructing the relative abundance of fine sediment transported in ancient channel networks.

APPENDIX

177 Supplemental data submitted.

ACKNOWLEDGMENTS

This research was supported by the donors of the American Chemical Society Petroleum Research Fund, NSF Awards #1455240 and #1935513 to E.H., and student support from the Geological Society of America, American Association of Petroleum Geologists, and Penn State Geosciences to N.W. Without the incredible expertise and generosity of SAFL personnel, particularly Ben Erickson and Sara Mielke, this work would not have been possible. We are grateful to E.

184 Chamberlin and Macalester College students for helping run experiments. We thank C. Paola, R.

Slingerland, T. Bralower, R. DiBiase, V. Ganti, S. Alpheus, E. Chamberlin, E. Greenberg, X. Hu,

S. Lyster, S. Trampush, and J. Walker for helpful discussions, and A. Fernandes, A. Ielpi, M.

Perillo, J. Pizzuto, P. Plink-Björklund, J. Shaw, and an anonymous reviewer for thoughtful and

constructive reviews.

FIGURE CAPTIONS

Figure 1. A) Diagram of experimental setup showing the location of clay and sand delivery; water entered the flume on the left side and exited over the weir on the right side. Sand was supplied dry and clay was delivered as a slurry from a mixing tank at a rate of 1 l/s, with different concentrations for each run. Reported data come from the active bed region. Measurement cart included sediment-sampling and ADV equipment; videos and photographs were taken from through the sidewall of the flume at 3.25 m. B) Example of bed evolution in the Test Section of the flume during the Intermediate Concentration run (3x vertical exaggeration). Lines show bed topography every 30 minutes (progressing from light green to dark green). Raw panel shows the full bed topography and the smoothed panel shows the same data averaged with a moving window of two average-bedform lengths (50 cm). Arrows indicate the approximate position of the front of the sediment wedge at each time. All runs showed the same bed evolution; complete bed-evolution histories and experimental details are included in supplemental material.

Figure 2. Example composite bed photos (A) from the glass sidewall of the flume and mapped

fines (B) from the end of the High Concentration Run; downstream is to the right. A) Sand appears dark gray and fine-sediment drapes and lenses appear white; clay-rich water during the high-concentration experiment appears light gray at the top of the panel. B) Fine-sediment accumulations were mapped from bed photos. Lenses (dark red) are areas of continuous fine-

207	sediment accumulations. Drapes (black) are thin horizons of fines-rich deposits often occurring or
208	bedform foresets and bedform-bounding surfaces. Interstitial fines (light gray) disseminated clay
209	that gives bed deposits an overall lighter-colored appearance than bed deposits lacking fines. White
210	dashed line shows the boundary between sediment that accumulated in the aggradational phase
211	(below) from the bypass phase (above). Gray-white striped region marks preserved portions of the
212	pre-run bed. Note horizontal scale difference from Figure 1B.
213	¹ GSA Data Repository item 202Xxxx, supplementary data including details of experimental
214	conditions and analyses, is available online at www.geosociety.org/pubs/ft20XX.htm, or on
215	request from editing@geosociety.org or Documents Secretary, GSA, P.O. Box 9140, Boulder,
216	CO 80301
217	REFERENCES CITED
218 219 220	Baas, J.H., Best, J.L., and Peakall, J., 2016, Predicting bedforms and primary current stratification in cohesive mixtures of mud and sand: Journal of the Geological Society, v. 173, p. 12–45, doi:10.1144/jgs2015-024.
221	Boggs, S.Jr., 2012, Principles of Sedimentology and Stratigraphy: Pearson.
222 223 224 225	Brewer, C.J., Hampson, G.J., Whittaker, A.C., Roberts, G.G., and Watkins, S.E., 2020, Comparison of methods to estimate sediment flux in ancient sediment routing systems: Earth-Science Reviews, v. 207, p. 103217, doi:https://doi.org/10.1016/j.earscirev.2020.103217.
226 227 228	Chamberlin, E.P., and Hajek, E.A., 2019, Using bar preservation to constrain reworking in channel-dominated fluvial stratigraphy: Geology, v. 47, p. 531–534, doi:10.1130/G46046.1.
229 230 231	Colombera, L., Arévalo, O.J., and Mountney, N.P., 2017, Fluvial-system response to climate change: The Paleocene-Eocene Tremp Group, Pyrenees, Spain: Global and Planetary Change, v. 157, p. 1–17, doi:10.1016/j.gloplacha.2017.08.011.
232 233 234 235	Dalrymple, R.W., and Choi, K., 2007, Morphologic and facies trends through the fluvial–marine transition in tide-dominated depositional systems: A schematic framework for environmental and sequence-stratigraphic interpretation: Earth-Science Reviews, v. 81, p. 135–174, doi:10.1016/j.earscirev.2006.10.002.

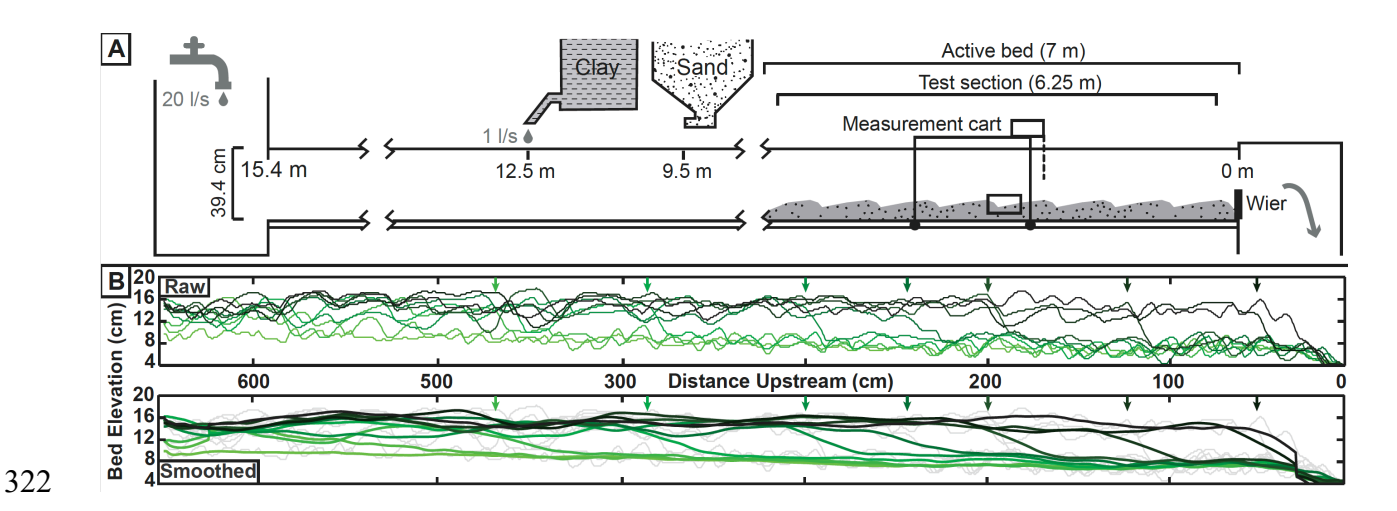
- Davies, N.S., and Gibling, M.R., 2011, Evolution of fixed-channel alluvial plains in response to Carboniferous vegetation: Nature Geoscience, v. 4, p. 629–633, doi:10.1038/ngeo1237.
- Dunne, K.B.J., and Jerolmack, D.J., 2020, What sets river width? Science Advances, v. 6, p. eabc1505, doi:10.1126/sciadv.abc1505.
- Foreman, B.Z., 2014, Climate-driven generation of a fluvial sheet sand body at the Paleocene-Eocene boundary in north-west Wyoming (USA): Basin Research, v. 26, p. 225–241,
- 242 doi:10.1111/bre.12027.
- Foreman, B.Z., Heller, P.L., and Clementz, M.T., 2012, Fluvial response to abrupt global warming at the Palaeocene/Eocene boundary: Nature, v. 491, p. 92–95,
- 245 doi:10.1038/nature11513.
- Ganti, V., Hajek, E.A., Leary, K., Straub, K.M., and Paola, C., 2020, Morphodynamic hierarchy and the fabric of the sedimentary record: Geophysical Research Letters, v. n/a, p.
- 248 e2020GL087921, doi:10.1029/2020GL087921.
- Ganti, V., Whittaker, A.C., Lamb, M.P., and Fischer, W.W., 2019, Low-gradient, single-threaded rivers prior to greening of the continents: Proceedings of the National Academy of Sciences, p. 201901642, doi:10.1073/pnas.1901642116.
- Ghinassi, M., Ielpi, A., Aldinucci, M., and Fustic, M., 2016, Downstream-migrating fluvial point bars in the rock record: Sedimentary Geology, v. 334, p. 66–96, doi:10.1016/j.sedgeo.2016.01.005.
- Hajek, E.A., Huzurbazar, S.V., Mohrig, D., Lynds, R.M., and Heller, P.L., 2010, Statistical Characterization of Grain-Size Distributions in Sandy Fluvial Systems: Journal of Sedimentary Research, v. 80, p. 184–192, doi:10.2110/jsr.2010.020.
- Hampson, G.J., 2016, Towards a sequence stratigraphic solution set for autogenic processes and allogenic controls: Upper Cretaceous strata, Book Cliffs, Utah, USA: Journal of the Geological Society, v. 173, p. 817–836, doi:10.1144/jgs2015-136.
- Hampson, G.J., Duller, R.A., Petter, A.L., Robinson, R.A.J., and Allen, P.A., 2014, Mass-Balance Constraints On Stratigraphic Interpretation of Linked Alluvial-Coastal-Shelfal Deposits From Source To Sink: Example From Cretaceous Western Interior Basin, Utah and Colorado, U.S.A: Journal of Sedimentary Research, v. 84, p. 935–960, doi:10.2110/jsr.2014.78.
- Ielpi, A., and Lapôtre, M.G.A., 2020, A tenfold slowdown in river meander migration driven by plant life: Nature Geoscience, v. 13, p. 82–86, doi:10.1038/s41561-019-0491-7.
- Lamb, M.P., de Leeuw, J., Fischer, W.W., Moodie, A.J., Venditti, J.G., Nittrouer, J.A., Haught, D., and Parker, G., 2020, Mud in rivers transported as flocculated and suspended bed material: Nature Geoscience, v. 13, p. 566–570, doi:10.1038/s41561-020-0602-5.

- Lapôtre, M.G.A., Ielpi, A., Lamb, M.P., Williams, R.M.E., and Knoll, A.H., 2019, Model for the
- Formation of Single-Thread Rivers in Barren Landscapes and Implications for Pre-
- 273 Silurian and Martian Fluvial Deposits: Journal of Geophysical Research: Earth Surface,
- v. 124, p. 2757–2777, doi:10.1029/2019JF005156.
- de Leeuw, J., Lamb, M.P., Parker, G., Moodie, A.J., Haught, D., Venditti, J.G., and Nittrouer,
- J.A., 2020, Entrainment and suspension of sand and gravel: Earth Surface Dynamics, v.
- 277 8, p. 485–504, doi:10.5194/esurf-8-485-2020.
- Lynds, R., and Hajek, E., 2006, Conceptual model for predicting mudstone dimensions in sandy braided-river reservoirs: AAPG Bulletin, v. 90, p. 1273–1288, doi:10.1306/03080605051.
- Martin, A.J., 2000, Flaser and wavy bedding in ephemeral streams: a modern and an ancient example: Sedimentary Geology, v. 136, p. 1–5, doi:10.1016/S0037-0738(00)00085-3.
- Matsubara, Y., Howard, A.D., Burr, D.M., Williams, R.M.E., Dietrich, W.E., and Moore, J.M.,
- 283 2015, River meandering on Earth and Mars: A comparative study of Aeolis Dorsa
- meanders, Mars and possible terrestrial analogs of the Usuktuk River, AK, and the Quinn
- 285 River, NV: Geomorphology, v. 240, p. 102–120, doi:10.1016/j.geomorph.2014.08.031.
- McMahon, W.J., and Davies, N.S., 2018, Evolution of alluvial mudrock forced by early land plants: Science, v. 359, p. 1022–1024, doi:10.1126/science.aan4660.
- 288 Mooneyham, C., and Strom, K., 2018, Deposition of Suspended Clay to Open and Sand-Filled
- Framework Gravel Beds in a Laboratory Flume: Water Resources Research, v. 54, p.
- 290 323–344, doi:10.1002/2017WR020748.
- Packman, A.I., and MacKay, J.S., 2003, Interplay of stream-subsurface exchange, clay particle
- deposition, and streambed evolution: Water Resources Research, v. 39,
- 293 doi:10.1029/2002WR001432.
- Peakall, J., Ashworth, P.J., and Best, J.L., 2007, Meander-Bend Evolution, Alluvial Architecture,
- and the Role of Cohesion in Sinuous River Channels: A Flume Study: Journal of
- 296 Sedimentary Research, v. 77, p. 197–212, doi:10.2110/jsr.2007.017.
- 297 Plink-Björklund, P., 2015, Morphodynamics of rivers strongly affected by monsoon
- 298 precipitation: Review of depositional style and forcing factors: Sedimentary Geology, v.
- 299 323, p. 110–147, doi:10.1016/j.sedgeo.2015.04.004.
- Reesink, A.J.H., Van den Berg, J.H., Parsons, D.R., Amsler, M.L., Best, J.L., Hardy, R.J., Orfeo,
- O., and Szupiany, R.N., 2015, Extremes in dune preservation: Controls on the
- completeness of fluvial deposits: Earth-Science Reviews, v. 150, p. 652–665,
- 303 doi:10.1016/j.earscirev.2015.09.008.
- Rust, B.R., and Nanson, G.C., 1989, Bedload transport of mud as pedogenic aggregates in
- 305 modern and ancient rivers: Sedimentology, v. 36, p. 291–306, doi:10.1111/j.1365-
- 306 3091.1989.tb00608.x.

Schieber, J., Southard, J., and Thaisen, K., 2007, Accretion of Mudstone Beds from Migrating Floccule Ripples: Science, v. 318, p. 1760–1763, doi:10.1126/science.1147001. Szupiany, R.N., Amsler, M.L., Hernandez, J., Parsons, D.R., Best, J.L., Fornari, E., and Trento, A., 2012, Flow fields, bed shear stresses, and suspended bed sediment dynamics in bifurcations of a large river: Water Resources Research, v. 48, doi:10.1029/2011WR011677. Wang, J., and Plink-Björklund, P., 2019, Stratigraphic complexity in fluvial fans: Lower Eocene Green River Formation, Uinta Basin, USA: Basin Research, v. 31, p. 892–919, doi:10.1111/bre.12350. Wilkerson, G.V., and Parker, G., 2011, Physical Basis for Quasi-Universal Relationships

Describing Bankfull Hydraulic Geometry of Sand-Bed Rivers: Journal of Hydraulic Engineering, v. 137, p. 739–753, doi:10.1061/(ASCE)HY.1943-7900.0000352.

Figure 1:



329 Figure 2:

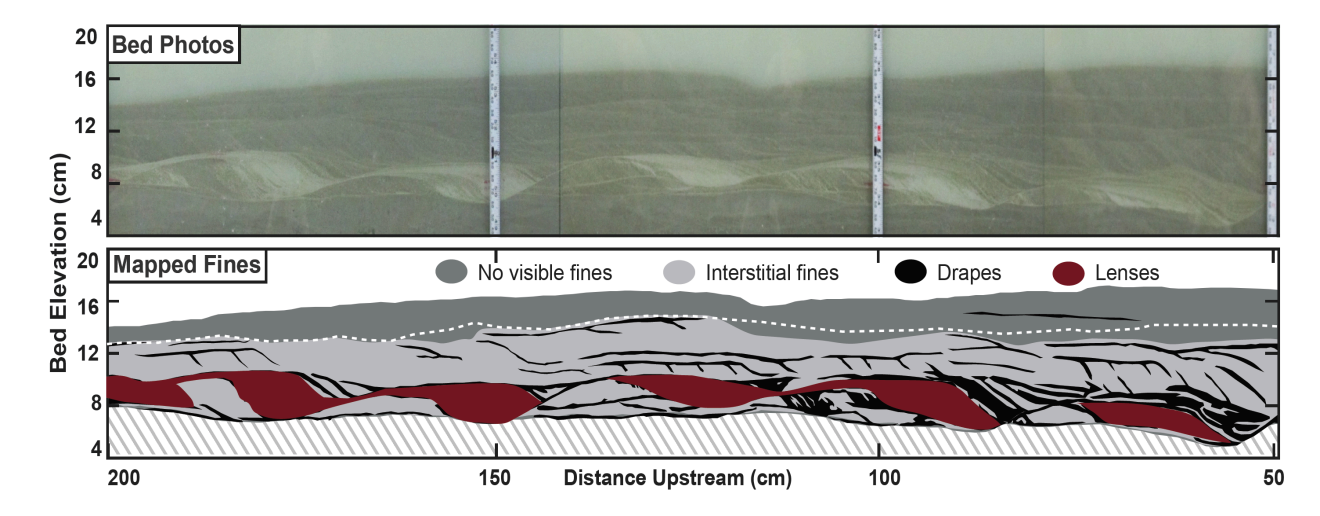


Table 1:

	sediment		eposits [% of total l adaional phase cro	Fines in bed samples [average wt%]			
	concentration	Interstitial	Drapes	Lenses	Expected	Aggradation	Bypass
High concentration	8500	40 (62)	12 (19)	6 (10)	0.17	2.2	0.4
Intermediate concentration	4000	34 (61)	8 (14)	0 (0)	0.08	0.8	0.2
Low concentration	1000	0 (0)	0.1 (0.1)	0 (0)	0.02	0.06	0.05
Intermittent discharge	1000	0 (0)	1 (1)	0 (0)	0.02	0.2	0.1

Table: Summary of experimental bed deposit characteristics. "Fine-sediment concentration" is the concentration of clay in the flow during each run. "Fine-sediment deposits" lists the percentage of bed cross-section exposed along the flume wall that contains intersitial fines, fine-sediment drapes, or fine-sediment lenses (e.g., Figure 2B); percent of each type of fine-sediment accumulation mapped within the aggradational phase of each experiment (below the white dashed line in Figure 2B) is shown in parentheses. "Fines in bed samples" is the average weight percent of bed samples from aggradational-and bypass-phase deposits of each run. "Expected" weight percent of fine sediment in bed samples is the amount of interstitial clay expected in bed pore waters (assuming 35% porosity) given the supplied fine-sediment concentration for each run. Full bed maps and sample data are included in the supplemental material, along with details of a constant-discharge control run that contained no supplied clay.

Data repository and supplemental information for Wysocki and Hajek: Mud in sandy riverbed deposits as a proxy for ancient fine-sediment supply

DESCRIPTION OF EXPERIMENTAL PROCEDURES	<u> 2</u>
Description of flume and sediment used in experiments	2
Startup and shutdown procedures	2
LINKS TO VIDEOS OF EACH EXPERIMENTAL RUN	4
EXPERIMENTAL CONDITIONS AND BED EVOLUTION	5
Table DR1: Summary of experimental conditions and bed evolution for each run.	5
Table DR2: Run and stop (settling) times for the Intermittent Discharge run	5 5
Figure DR1: Bed aggradation throughout each run	6
Figure DR2: Histogram of measured bedform heights for each run	6
Experimental sediment-transport conditions	7
Figure DR3: Shield's diagram (after Wilkerson and Parker, 2011) showing experimental sediment-	-
transport conditions	7
Fine sediment transport	7
Comparison with of experimental conditions with studies	8
Table DR3: Comparison of conditions in this study with other mixed sand-clay flume experiments	8
Figure DR4: Comparison of flow conditions in experiments from this study to the phase diagram	0
presented in Baas et al. (2009) Figure DR5: Comparison of experiments in this study to the clay flow phase diagram of Baas et al.	9
(2009)	9
	10
	11
·	12
	12
	13
DED DEI OSIT SIMILEING	13
Table DR4: Bed-deposit sample locations and weight percent of clay in the sample	13
	14
	14
Figure DR 11: Potential fine-sediment yield from settling given effective particle size and bed-	
	14
DEPOSIT CHARACTERISTICS AND CLAY ACCUMULATIONS	<u> 16</u>
Table DR5: Experimental deposit characteristics and clay-mapping results.	16
	16
Figure DR12: Photographs and mapped clay accumulations of each run as seen through the glass	
wall of the flume.	16
REFERENCES	19

DESCRIPTION OF EXPERIMENTAL PROCEDURES

Description of flume and sediment used in experiments

Experiments were conducted in the 24-in general purpose flume at the St. Anthony Falls Laboratory, University of Minnesota (http://www.safl.umn.edu/facilities/general-purpose-flumes-6-inch-20-inch-24-inch-flumes); see Figure 1 in the main manuscript. The flume is a feed style flume 15.42 meters long (50 ft) and 39.97 cm deep (15.5 in). Near the head box the flume is 61 cm and between 14.7 and 12.2 m, the flume narrowed from 61 cm to 30.5 cm. The flume was 30.5 cm-wide for from 12.2 m to the end (0 m) at the weir. The weir height for all runs was fixed at 16 cm. For each run, the initial sediment wedge extended from the outlet of the flume to 8 m and was graded to a slope of 0.004.

The sand feeder was positioned at 8.5 m and the sand feed rate was set at 15.0 g/s (a voltage of 356 on the auger box). This feed rate was verified before each run and prior to sand feed being turned off at the conclusion of each run. Based on water velocity and fall velocity of the median grain diameter sand (0.323 mm) the sand traveled 1.5-1.75 m before reaching the bed. The sand used in these experiments is AGSCO #40-#70 silica sand. This has a narrow distribution with D_{50} =0.323 mm, and a sorting coefficient of 1.2. A board was positioned below the feeder to disperse the sand supply, spreading it across the width of the flume.

Clay was delivered to the flume via two mixing tanks. First, clay was fully mixed and wetted in a mixing tank located on the floor above the flume. A clay slurry left this initial mixing tank and was delivered to a second 1 m³ mixing tank positioned just above the flume at 12.5 m. In the second mixing tank, the clay slurry was diluted with city water supplied at a rate of 1 L/s and was mixed via propeller. The dilute clay mixture from the secondary mixing tank was then introduced to the flume at a rate of 1 L/s. Clay was added to the initial mixing tank in volumes that produced the desired final concentration (21 g/L slurry for the Low Concentration and Intermittent Discharge runs, 85 g/L slurry for the Mid-concentration run, and ~179 g/L slurry for the High Concentration run), and the clay slurry was delivered to the secondary mixing tank at a rate to balance the 1 L/s discharge from the secondary mixing tank into the flume. The water level in the tank and sediment feed rate (especially when high) were variable and were monitored and adjusted frequently throughout the course of each run to maintain the appropriate clay concentration in the flume. The clay feed from the secondary take was run over a board to disperse the clay supply uniformly across the width of the flume; this also helped prevent the slurry from becoming a density flow. Clay used in this experiment was Cary Snobrite kaolin clay with a median grain diameter of 0.004 mm. There was no overlap between sand and clay grain size distributions.

The main water supply to the flume Mississippi River water sourced from the St Anthony Falls Lab main channel diversion.

Startup and shutdown procedures

Start-up checklist

- Set initial sediment wedge by scraping off all sediments from prior experiments and grading the slope at 0.004.
- Test sand and clay sediment feed rates.
- Wet sediment wedge for over an hour so that water fills all pore spaces. Using a very low discharge, slowly fill the flume to the level of the weir.
- Start camera.

- Increase the flow to the desired discharge. Lift up on hydraulic pump until plate is at correct location (marked).
- Start clay slurry feed.
 - o Turn on hose and sediment feeder in secondary clay mixing tank.
- Turn on sand feed. This starts the official time.
- Note: Ideally clay and sand are turned on at the same time. This can be done with more than one person. The person downstairs turns the hose on, the person upstairs turns the clay feeder on then opens the ball valve. When the slurry enters the flume, the person downstairs turns on the sand feed.
- Check discharge by the water level going over the weir. Should be at 29 cm. if not, adjust discharge with hydraulic pump.

Shut down procedures

- Note time when sediment wedge reaches the weir and the entire bed is at bypass.
- Continue run for 15-30 minutes after this time and begin shut-down.
- Slightly decrease discharge so sand is no longer in suspended load regime.
- Turn off sand feed.
- Turn off clay feed.
 - o Shut ball valve, turn off hose, turn off sediment feeder.
- Immediately turn off river water discharge.
- Open drain on the headbox so the flume slowly drains from both sides.
- When bed is drained (still water in the flume, just not above the bed surface) open drain on headbox fully to allow flume to fully drain.
- Turn fan on the bed. Fan is attached to the top of the flume with clips at 1.5 meters blowing upstream.
- Let bed dry over two nights.

Procedures during run

- Collect velocity measurements at 6/10 water depth for 5-10 minutes.
- Collect additional velocity profiles by measuring for one minute at increments of 2 cm water depth from the bed to the top of the flow. (This proved difficult with migrating bedforms.)
- Collect bed and water surface elevation measurements from measuring tape every 50 cm of the test section. Make water surface elevation measurements every 1
- Take photographs of the test section every 30 minutes (15 minutes after bed and water surface elevations).
 - O These are taken 180 cm (~6 ft) away from the flume at points (for the left foot of the tripod) marked on a piece of tape on the floor.
- Suspended sediment samples

meter outside of the test section.

 Samples are taken every 30 minutes by a rake of suspended sediment samplers (Photo), with active tubes spaced 5 cm apart.

Photo: Suspended sediment sampler

O Suspended sediment sample are collected at the 2 m position in the flume from 3 cm, 8 cm, and 13 cm above the bed.

- Samples are taken by siphoning water through tubes and letting water enter 16 oz containers
- Nearest dune location and dune height are noted
- Active bed material samples
 - o Grab samples are taken every 30 minutes (with suspended sediment samples) taken with 8 oz containers.
 - o Taken from top few centimeters of closest upstream dune to the 2 m position in the flume.
- Note the time when the prograding wedge reaches the weir and the entire bed is at bypass.
- Continue run for 15- 30 minutes.

Shutdown and startup procedures for variable flow run

- Follow shut-down procedures as normal with the exception of only turning down the clay feed before turning the river water off. Immediately after river water is turned off, shut down clayfeed and let the bed slowly drain naturally. Do not open the valve in the headbox.
- Allow clay to settle for prescribed time.
- To start flume, turn on clay feed to a very low discharge and slowly increase river water discharge (so as not to send a flood wave through the flume eroding the bed). When river discharge is up, turn on clay and sand feed as normal.

LINKS TO VIDEOS OF EACH EXPERIMENTAL RUN

High Concentration Run:

https://www.youtube.com/watch?v=94O93QsWivU https://www.youtube.com/watch?v=_hLRHIdaPxI

Intermediate Concentration Run:

https://www.youtube.com/watch?v=wtui5OUFGvwhttps://www.youtube.com/watch?v=nTdUC84508Y

Low Concentration Run:

https://www.youtube.com/watch?v=-fE8 mEmQ0Q

Intermittent Discharge Run:

https://www.youtube.com/watch?v=N4nBBHzqulE https://www.youtube.com/watch?v=XZfngqdCwZ8

EXPERIMENTAL CONDITIONS AND BED EVOLUTION

Table DR1: Summary of experimental conditions and bed evolution for each run.

Aggradation time is the total time the experiment experienced a net increase in average bed elevation in the test section (starting from the beginning of the experiment) and bypass time is the total time the experiment was run after the bed in the test section fully aggraded (i.e. no net increase in mean bed elevation).

	No Fines	Low Concentration	Intermediate Concentration	High Concentration	Intermittent Discharge				
		EXPERIMENT	AL CONDITIONS						
Water discharge (l/s)	21	21	21	21	21 with pauses of 0 (see Table DR2)				
Sand discharge (g/s)	15.0	15.0	15.0	15.0	15.0 (when water discharge > 0)				
Clay concentration (mg/l)	0	1,000	4,000	8,500	1,000				
Total run time (min)	303	272	277	253	262				
Aggradation time (min)	239	239	262	236	247				
Bypass time (min)	64	33	15	17	15				
	BED EVOLUTION								
Bed aggradation rate (cm/min)	0.024	0.025	0.025	0.025	0.024				
Total bed aggradation (cm)	6.1	6.1	6.8	6.4	6.6				
Downstream wedge progradation rate (cm/s)	2.4	2.4	2.1	2.8	2.1				
Mean bedform height (cm)	2.3	2.5	2.2	2.3	2.2				
Bedform height standard deviation	1.5	1.4	1.4	1.2	1.2				
Mean bedform migration rate (cm/s)									
Aggradational Phase		1.1	1.1	1.8	1.2				
Bypass Phase		12.0	8.6	11.1	10.2				

Table DR2: Run and stop (settling) times for the Intermittent Discharge run

	Part 1	Part 2	Part 3	Part 4	Part 5
Run time (min)	59	55	56	66	27
Settling time (water	69	69	1010	179	End of run
discharge = 0; min)					

Figure DR1: Bed aggradation throughout each run

Bed elevation is the mean elevation of the bed (e.g., mapped profiles in Manuscript Figure 1 and Figure DR6). High = High Concentration Run, Int = Intermediate Concentration Run, Low = Low Concentration Run, Var = Intermittent Discharge Run, Nf = No Fines (control) Run.

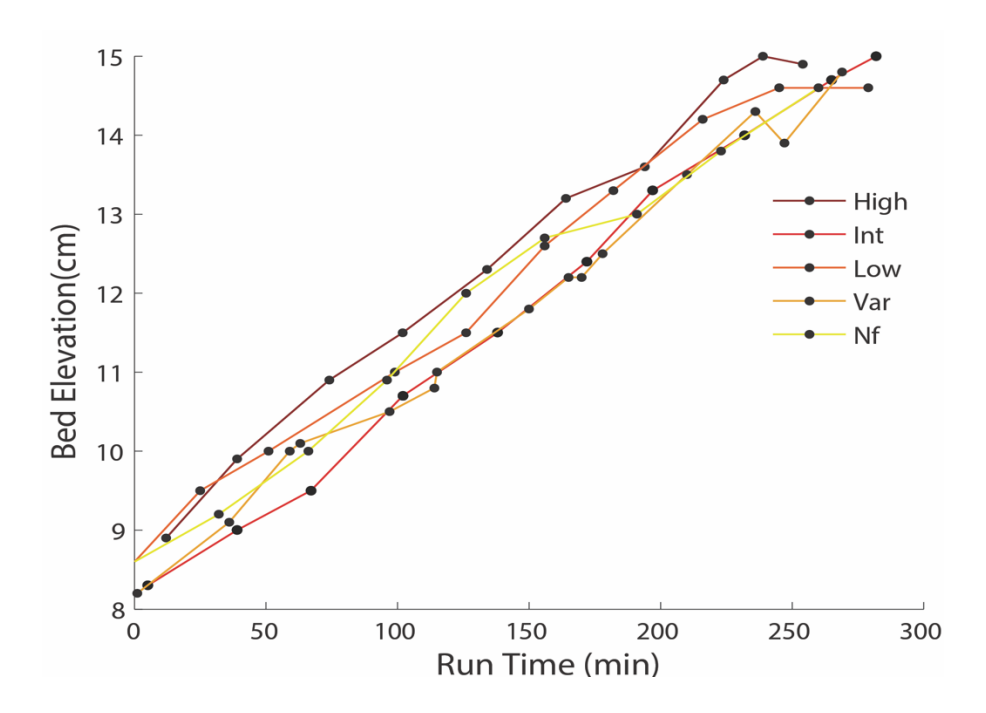
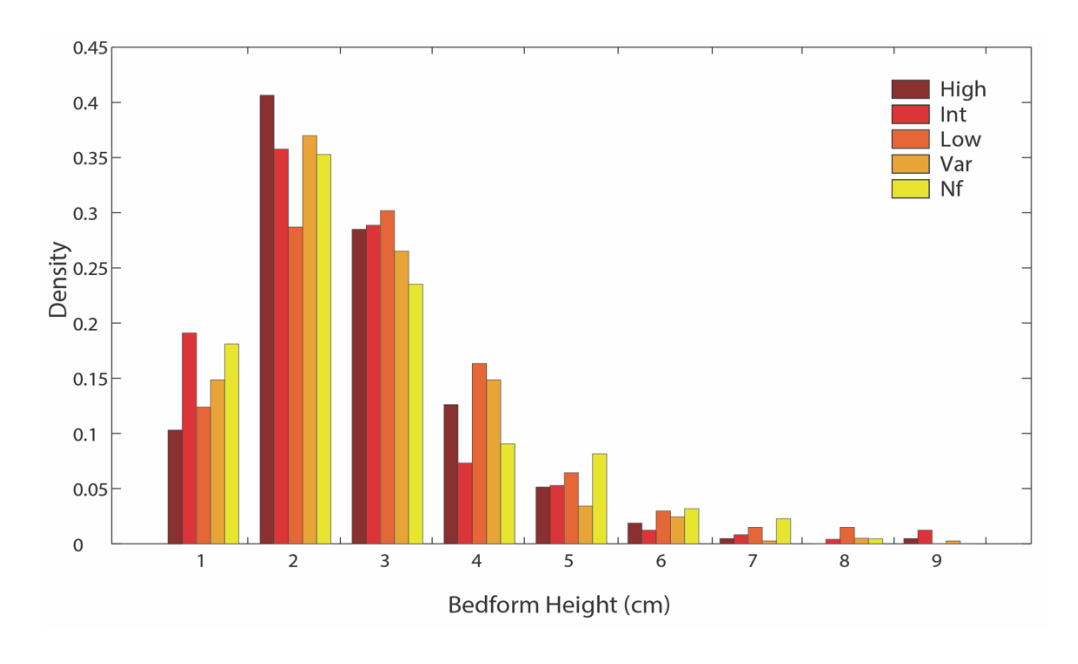


Figure DR2: Histogram of measured bedform heights for each run

On bed-topography profiles mapped from photos every 30 mins throughout the experiment (Figure DR4), the height (elevation of crest minus elevation of trough) and length (distance between dune crests) of each bedform was measured. Number of bedforms measured for each experiment: No Fines (NF) = 188, Low Concentration (Low) = 202, Intermediate Concentration (Int) = 246, High Concentration (High) = 214, Intermittent Discharge (Var) = 420.



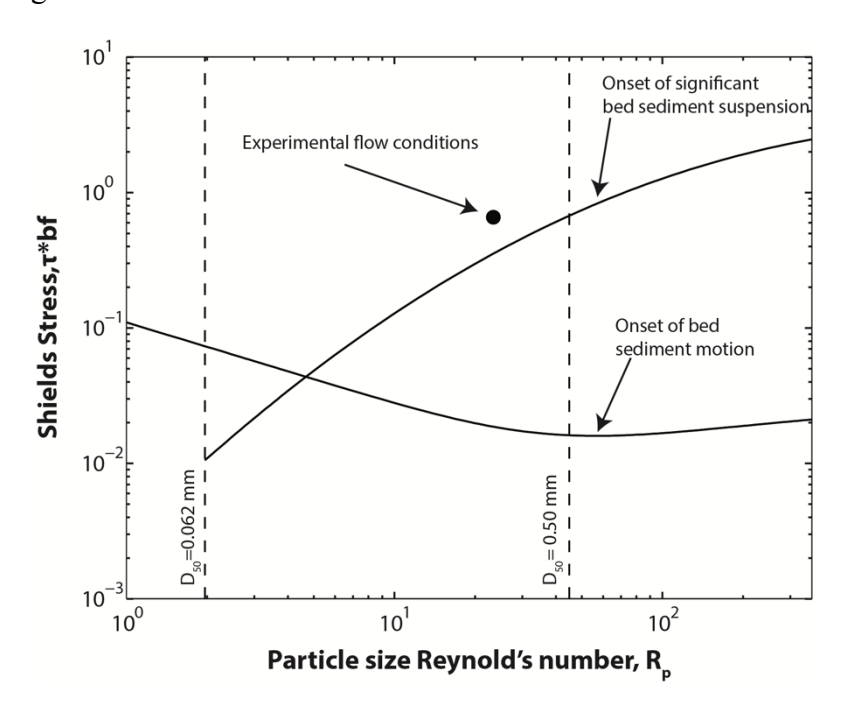
Experimental sediment-transport conditions

Figure DR3: Shield's diagram (after Wilkerson and Parker, 2011) showing experimental sediment-transport conditions

Shields Stress (τ_{bf}^*) was calculated using Wilkerson and Parker's Equation 13:

$$\tau_{bf}^* = \frac{H_{bf}S}{RD_{50}}$$

where H_{bf} is the flow depth, S is the slope, R is the submerged specific gravity of sediment, and D_{50} is the median grain size.



Fine sediment transport

Fine sediment supplied to the flume should have been easily suspended and not settled within the length of the flume. Given the slowest average water velocity in the suite of experiments (40 cm/s), and a settling velocity for clay in freshwater of 0.0002 cm/s (Sutherland et al., 2015), clay introduced at 12.5 m in the flume would have settled only 60 microns through the water column during its transport downstream in the experiments. Additionally, the concentration of clay in these experiments (0.5% by weight) was lower than the concentrations shown to induce significant changes in settling behavior of clay (either through flocculation or hindered settling (e.g., Sutherland et al., 2015) or the turbulence character of the flow (e.g., Baas et al., 2009). The potential role of fine-sediment transport via flocculated or aggregated particles in these experiments is discussed in Figures DR9 and DR10.

Comparison with other experimental studies

Table DR3: Comparison of conditions in this study with other mixed sand-clay flume experiments

Values for experiments in this study are averages of measurements taken throughout each run. Concentration (C) was imposed in each run. Flow depth (h) for each run is the average water-surface elevation minus the average bed elevation. Average flow velocity (U) was estimated by averaging ADV measurements throughout each run. Slope is the average of measured water-slopes during each run. Froude (Fr) and Reynolds (Re) numbers are estimated using flow depth and velocity and standard values for water density and viscosity. Baas et al. experiments include those that match the experimental conditions of this study most closely. Baas et al. classify the flow structure of their runs using detailed Ultrasonic Doppler velocimetry profiling (listed in Notes column). All data were reported in their 2009 and 2011 papers; slope value for the 2011 run is a bed slope. For Packman and MacKay experiments, slope is reported as "energy grade line"; Fr and Re were not reported in their paper, so we estimated values for each run (italics).

	Run	C (mg/l)	h (cm)	U (cm/s)	Slope	Fr	Re	Notes
	No Fines (control)	0	17.5	45	0.0018	0.34	78750	
XX /	Low Conc.	1000	16.6	50	0.0019	0.39	83000	Variable Flow
Wysocki & Hajek (this study)	Intermed. Conc.	4000	15.1	40	0.0016	0.33	60400	Run values are for high flow
study)	High Conc.	8500	14.9	60	0.0019	0.50	89400	conditions
	Intermittent Flow	1000	16.2	46	0.0020	0.37	74520	
Baas et al. (2011)	1	5200	15.1	46.5	0.00138	0.38	69939	Turbulent Flow
	3-1	500	14.5	43.9	0.00018	0.37	63599	Turbulent Flow
	3-2	4000	15.7	42.6	0.00029	0.34	65256	Turbulent Flow
Baas et al. (2009)	3-3	9600	15.5	41.4	0.00029	0.34	63473	Turbulence- Enhanced Transitional Flow
(4-2	4000	15.4	55.9	0.00029	0.44	86023	Turbulent Flow
	4-3	9800	15.1	55.7	0.00029	0.43	83182	Turbulent Flow
	5-2	4200	15.0	70.4	0.00029	0.58	105467	Turbulent Flow
Packman	1	230, 460, 230	8.7	23.3	0.064	0.25	20271	Pulsed injections of clay
and MacKay	2	280, 230, 220	11.8	23.7	0.044	0.22	27966	Pulsed injections of clay
(2003)	3	810	8.6	23.6	0.064	0.26	20296	Pulsed injection of clay

Figure DR4: Comparison of flow conditions in experiments from this study to the phase diagram presented in Baas et al. (2009)

Approximate range of experiments in this study shown in the gray box. Note that their diagram is for flow depths from 0.13-0.16 m, and that some of our experiments are slightly above those depths. Baas et al. Figure 17.

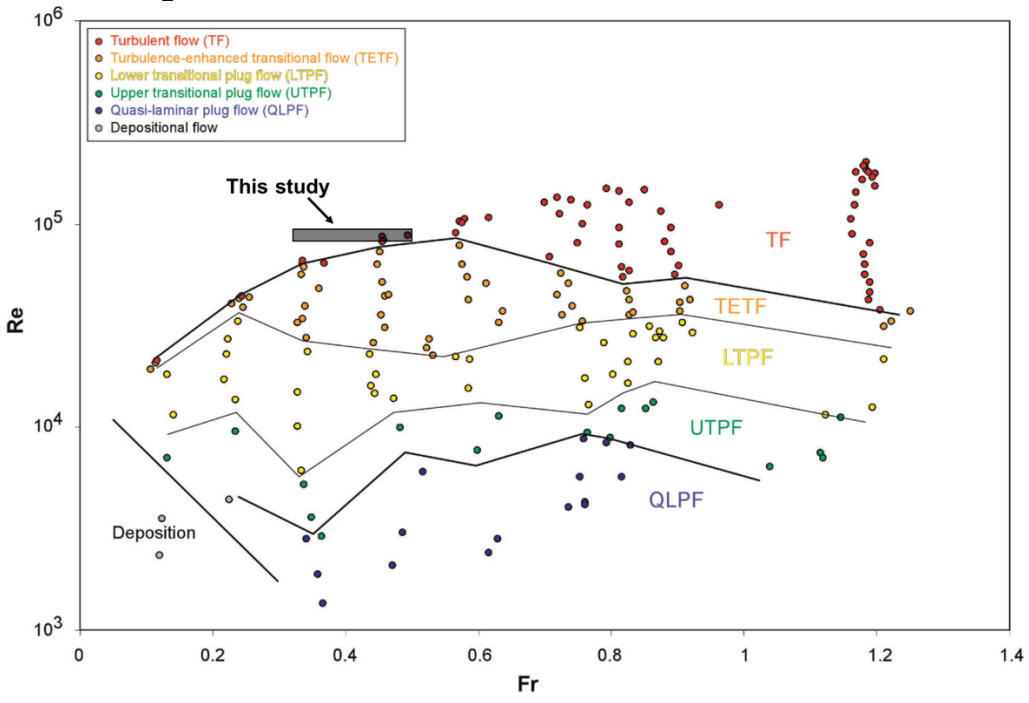


Figure DR5: Comparison of experiments in this study to the clay flow phase diagram of Baas et al. (2009)

Approximate range of experiments in this study is shown in the orange box. U is the depth-averaged flow velocity and C is the depth-average volume concentration of clay. Baas et al. Fig 15A.

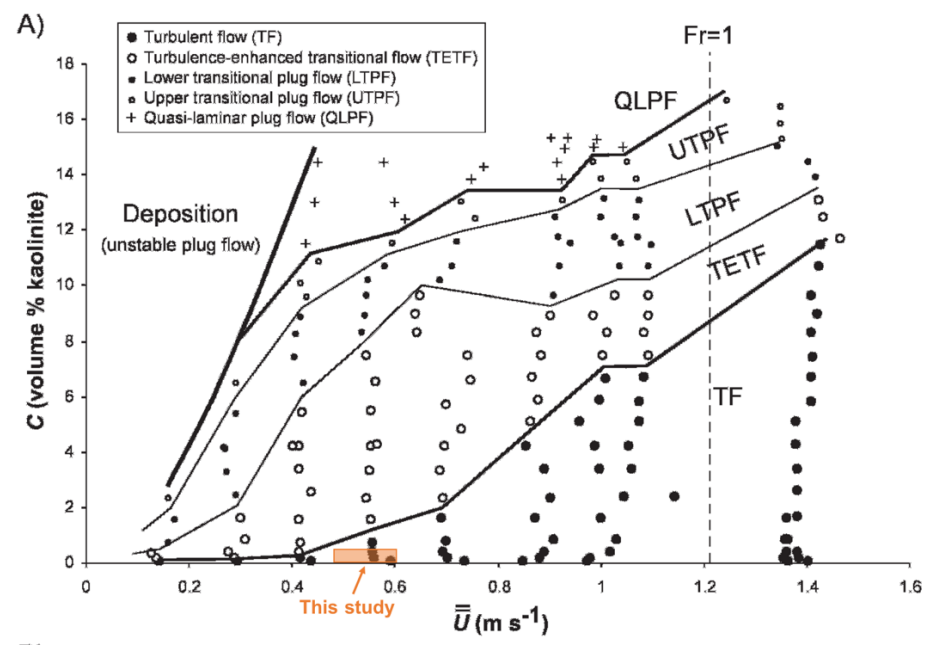


Figure DR6: Topographic profiles through time of each experiment

The top figure in each set is the measured values and the bottom figure is smoothed profiles, which is accomplished with a moving window two average dune lengths (50cm); colors show profiles every 30 minutes (light to dark, as in Manuscript Figure 1). Vertical exaggeration is 3x. Variable Flow refers to the Intermittent Discharge experiment.

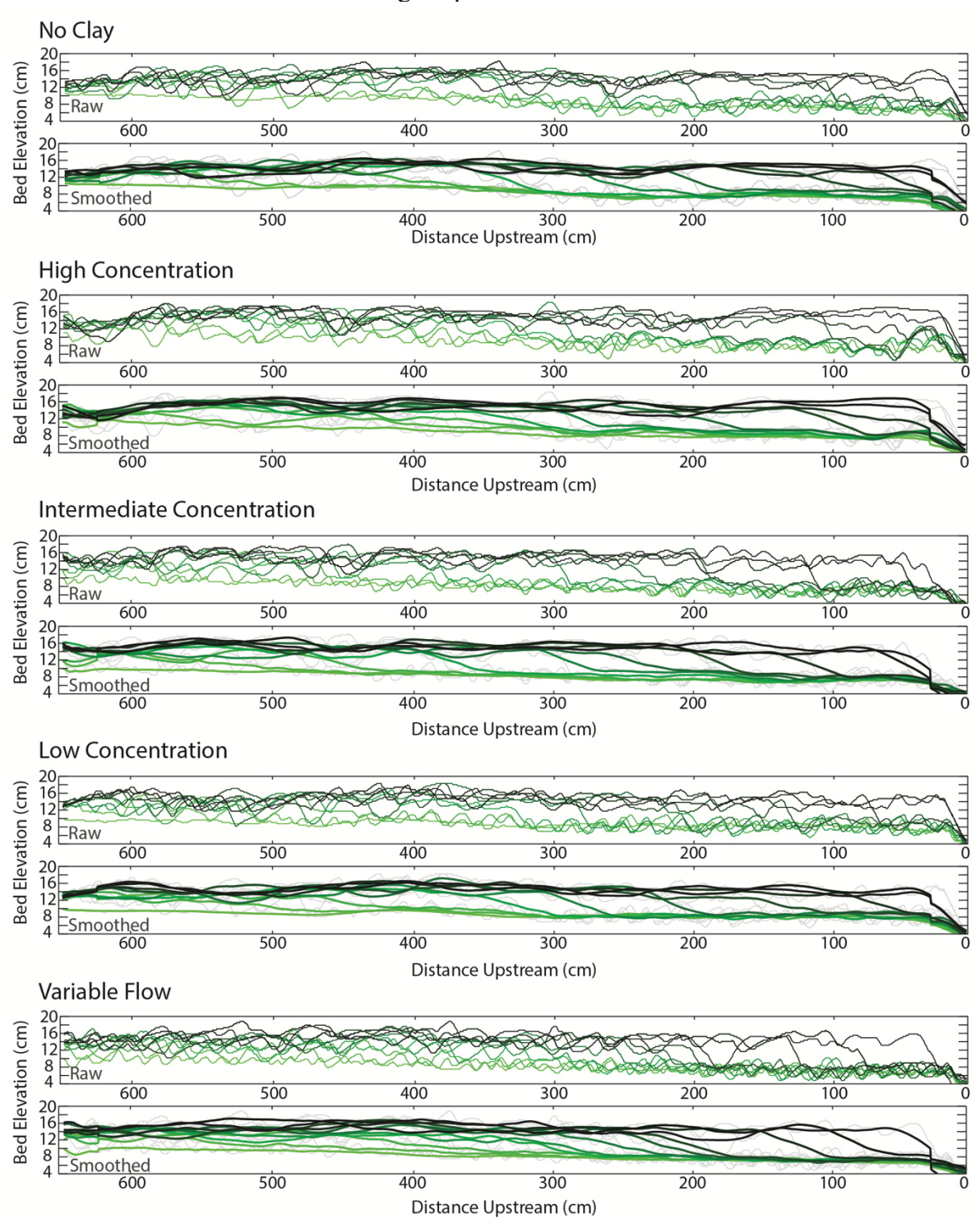
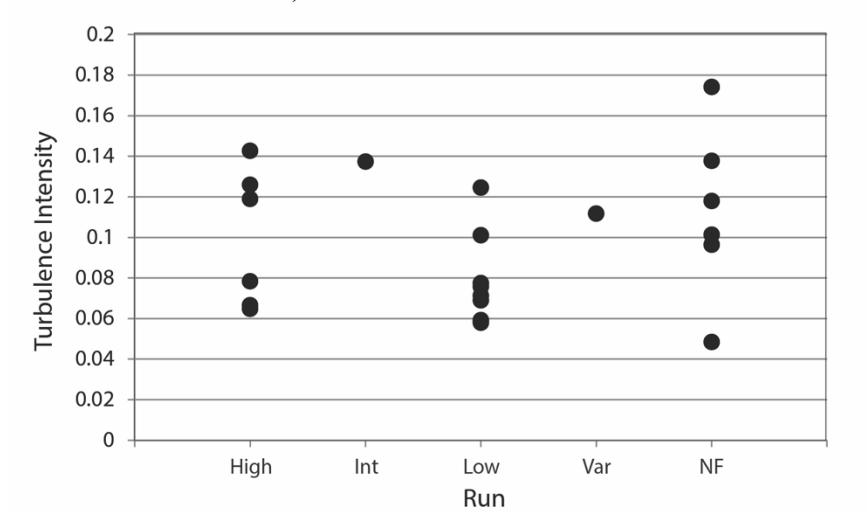


Figure DR7: Turbulence intensity calculated from ADV data from each run

There is no evidence of damping of turbulence at high clay concentration. (High = high concentration, Int = intermediate concentration, Low = low concentration, Var = intermittent discharge, NF = no fines control run.)



WinADV was used to process ADV data. Data were filtered using the automatic despiking program and used to calculate Turbulence Intensity (TI):

$$TI = \frac{u'}{U} = \frac{\sqrt{\frac{1}{3} \left(u_x'^2 + u_y'^2 + u_z'^2 \right)}}{\sqrt{U_x^2 + U_y^2 + U_z^2}}$$

where u' is the root mean square of the turbulent velocity fluctuations and U is the mean velocity (following, e.g., Bridge and Demicco, 2008).

Figure DR8: Suspended sediment concentration profiles

Experiments show a generally well-mixed clay concentration throughout the water column. Clay concentration varies during a run, but there was no overlap in clay concentration between runs. (High = high concentration, Int = intermediate concentration, Low = low concentration, Var = intermittent discharge.)

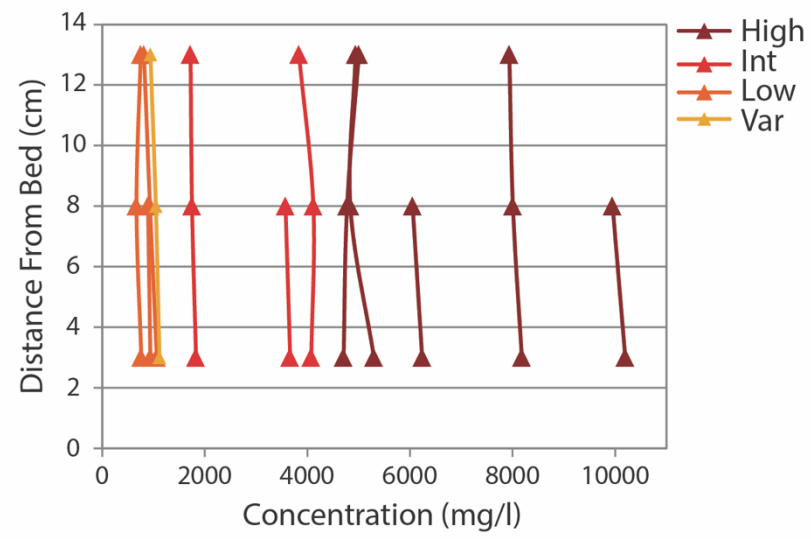
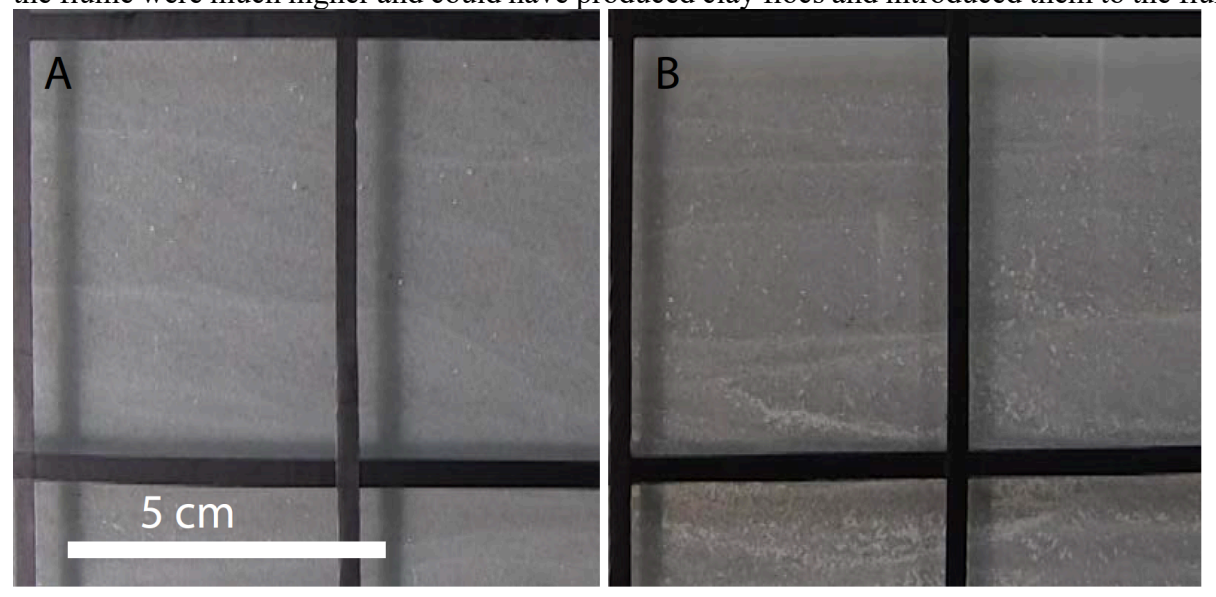


Figure DR9: Example images of clay aggregates in experimental runs.

Kaolinite flocs (white dots) in both the low-concentration run (A) and in the high-concentration run (B). Along the flume wall, in videos, there was evidence of flocculation in all runs, with more in the high-concentration experiment. Flocculation may have created a clay bed-material load by generating particles large enough to behave like sand. The constant clay-concentration profiles with depth (Figure DR8) contrast with the expected increase in clay concentration with depth if the majority of fine sediment were being transported as larger aggregates (Lamb et al., 2020). Clay concentrations in the flume (freshwater with clay concentrations <0.5 wt %) were below thresholds for significant flocculation documented in other experiments (e.g., > 3.0 wt % in still, fresh water in Sutherland et al. (2015)). However, concentrations in the mixing tank used to introduce clay to the flume were much higher and could have produced clay flocs and introduced them to the flume.



BED DEPOSIT SAMPLING

After each experiment, the bed was slowly drained and allowed to dry for two days prior to excavation. At this point the bed was dry enough to excavate without collapsing. Bed-deposit samples and photographs were taken from the middle of the flume at various locations at different depths (Table DR4 and Figure DR10) in order to capture samples deposited during both bypass and aggradation phases. These samples were taken with a 7cm x 7cm excavator tool, which allowed for bulk sediment samples in a manner analogous to hand-sample collection of bed-material deposits from ancient outcrops. Bed-deposit samples were then wet-sieved to determine the fraction of clay.

Table DR4: Bed-deposit sample locations and weight percent of clay in the sample

Depositional phase and type of clay accumulations captured by each sample are noted. Qualitative sample descriptions describe the nature sample after being oven dried. Sands in some samples were clumped together and had to be manually disaggregated after sampling, indicating abundant clay. The NF run was a control experiment conducted with no clay discharge. Clay-sized material detected in that run came from the water (supplied from the Mississippi River via the St. Anthony Falls Lab main-channel diversion) or residuum within the sand supply. (Var = intermittent flow)

Sample number	Run	Location (m)	Depth (cm)	Total weight (g)	Clay weight (g)	Clay %	Phase and clay types captured	Qualitative sample description	
NF-1	NF	2.00	12.5-15.5	536.56	0.06	0.011	bypass	loose sand	
NF-2	NF	2.00	9.5-12.5	523.92	0.08	0.015	aggradation	loose sand	
NF-3	NF	5.00	12.0-15.0	491.25	0.07	0.014	bypass	loose sand	
H-1	High	2.80	11.5-14.5	748.70	5.22	0.697	bypass	sticky/clumpy	
H-2	High	2.80	8.5-11.5	825.56	16.87	2.044	aggradation. Clay drapes	hard	
H-3	High	5.60	11.5-14.5	692.41	2.22	0.321	bypass	sticky/clumpy	
H-4	High	5.60	8.5-11.5	778.64	2.46	0.316	bypass	sticky/clumpy	
H-5	High	1.70	7.0-10.0	787.79	33.37	4.236	aggradation. Part of clay rich lens	hard	
I-1	Int	3.35	11.5-14.5	716.00	1.50	0.210	bypass	loose with clumps	
I-2	Int	3.35	8.0-11.0	833.63	3.47	0.416	split	sticky/clumpy	
I-3	Int	2.35	11.0-14.0	783.41	2.25	0.288	bypass	loose with clumps	
I-4	Int	2.35	7.0-10.0	859.58	15.58	1.813	aggradation. Clay drapes	hard	
I-5	Int	4.60	12.5-15.5	700.41	1.46	0.209	bypass	loose with clumps	
I-6	Int	4.60	8.5-11.5	901.94	1.97	0.218	split	loose with clumps	
L-1	Low	1.80	11.0-14.0	746.79	0.35	0.047	bypass	loose sand	
L-2	Low	1.80	7.5-10.5	799.44	0.51	0.064	aggradation	loose sand	
L-3	Low	4.10	11.0-14.0	824.75	0.38	0.046	bypass	loose sand	
L-4	Low	5.50	11.0-14.0	419.72	0.23	0.055	split (mostly bypass)	loose sand	
V-1	Var	3.70	11.5-14.5	717.34	0.43	0.060	bypass	loose sand	
V-2	Var	3.70	8.0-11.0	871.74	2.00	0.229	aggradation. Part of clay drape	loose sand with clumps	
V-3	Var	5.25	11.5-14.5	778.63	0.51	0.065	bypass	loose sand	
V-4	Var	5.25	8.5-11.5	791.50	0.74	0.093	aggradation	loose sand	
V-5	Var	2.00	7.5-10.5	896.84	1.74	0.380	aggradation. Part of clay drape	loose sand with clumps	

Expected clay weight percent in bed deposits

The expected weight percent of clay in the bed ($E_{wt\%clay}$; Table in the main manuscript) is the percent mass of interstitial clay that could be present in bed pore space given the supplied clay concentration in the flow (C_{clay}), bed porosity (f_{pore} ; assumed to be 0.35 after Beard and Weyl (1973), and density of sand ($\rho_{quartz} = 2.65 \text{ g/cm}^3$).

$$E_{wt\%clay} = \left(\frac{C_{clay}f_{pore}}{C_{clay}f_{pore} + \rho_{quartz}(1 - f_{pore})}\right) \times 100$$

Figure DR10: Comparison with Lamb et al. (2020) & de Leeuw et al. (2020)

Experimental results from this study compared with modern river data from Lamb et al. (2020) and de Leeuw et al. (2020). Lamb et al./de Leeuw et al. data tables were filtered for rivers with fine sediment (<16.5 micron, approximating the coarse tail of the kaolin clay supplied in these experiments) reported in both bed and suspended-sediment samples (Ganges and Yellow rivers). Mass fraction in bed is the total mass reported of particles <16.5 micron in bed samples. Mud suspended sediment volume concentration is the average overall suspended sediment concentration weighted for the fraction of suspended sediment that is <16.5 microns. Wysocki and Hajek experimental values show the average suspended sediment concentration supplied to the experimental runs and the average bed mass fraction found in bed-deposits samples from both the aggradation and bypass phases of the experiments. Available modern river data show the same overall trend of increasing mud in the bed for higher suspended-sediment concentrations. Expected weight percent of clay $E_{wt\%clay}$ is estimated as shown in the preceding section.

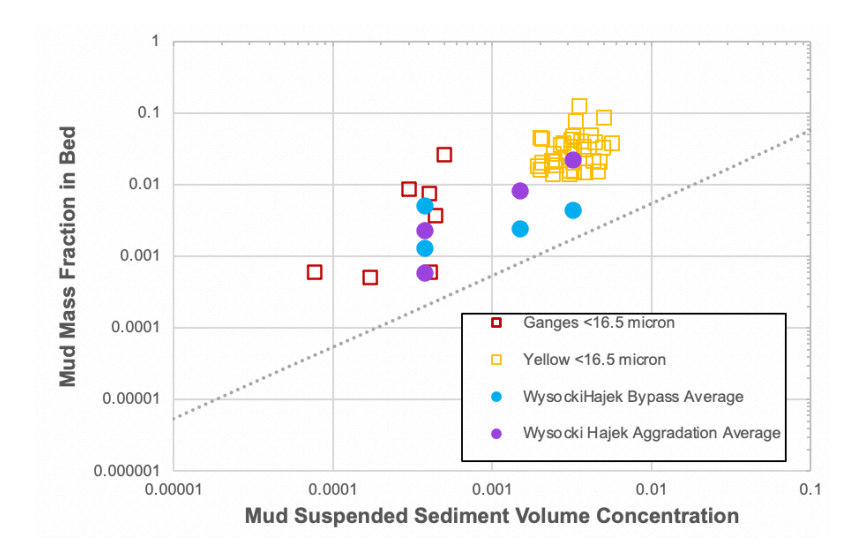


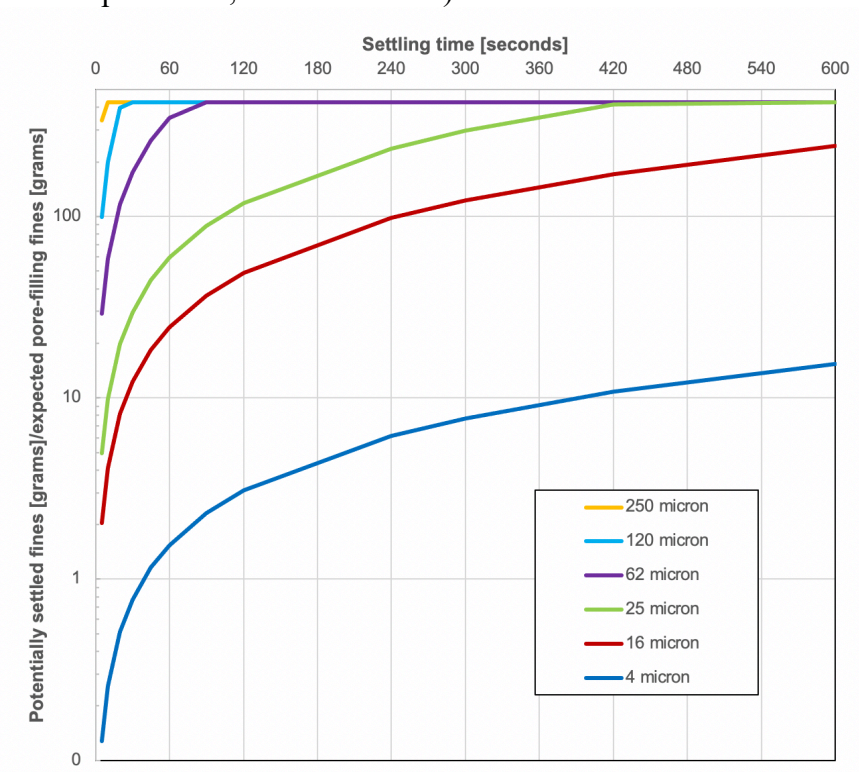
Figure DR 11: Potential fine-sediment yield from settling given effective particle size and bed-reworking period

Although the settling velocity of fine silt and clay is slow, settling could contribute significant fines to bed deposits, particularly if bedform migration rates (i.e. bed reworking periods) were slow and/or fine-sediment transport was dominated by flocs or aggregates with higher settling rates. To compare the potential for settling to explain the difference in fine-sediment retention between the aggradational and bypass phases of our experiments, we compared the degree to which bed-

reworking period could allow significant fine sediment to accumulate in bed deposits for a range of effective grain sizes.

Potential fine sediment yield from settling is normalized by the expected mass of pore filling-fines (see **Expected clay weight percent in bed deposits**, above) for the low-concentration run (1000g/mL). Potentially settled fines were estimated as the amount of fine sediment that could settle on a 1 mm² patch of bed over a given time period (Settling time), given a settling velocity determined by an effective grain size (assuming density = 2.65 g/cm³). Maximum values are limited by experimental flow depths of 15 cm (i.e. if settling velocity would be high enough to exceed 15 cm for a given settling time, the potential amount of fines settling in a 15 cm water column was assumed).

Bed reworking period, the average time between successive bedform scours passing a given location, is estimated as 10.8 mins (648 sec) for the aggradational phase and 1.3 mins (78 sec) of the experiments. (Bedform lengths in the experiments were ~14 cm and average bedform-migration rate was 1.3 cm/min for the aggradational phase and 10.5 cm/min for the bypass phase of the experiments; see Table DR1.)



DEPOSIT CHARACTERISTICS AND CLAY ACCUMULATIONS

Table DR5: Experimental deposit characteristics and clay-mapping results.

5.0
3.2
5230
3250
2010
0.62

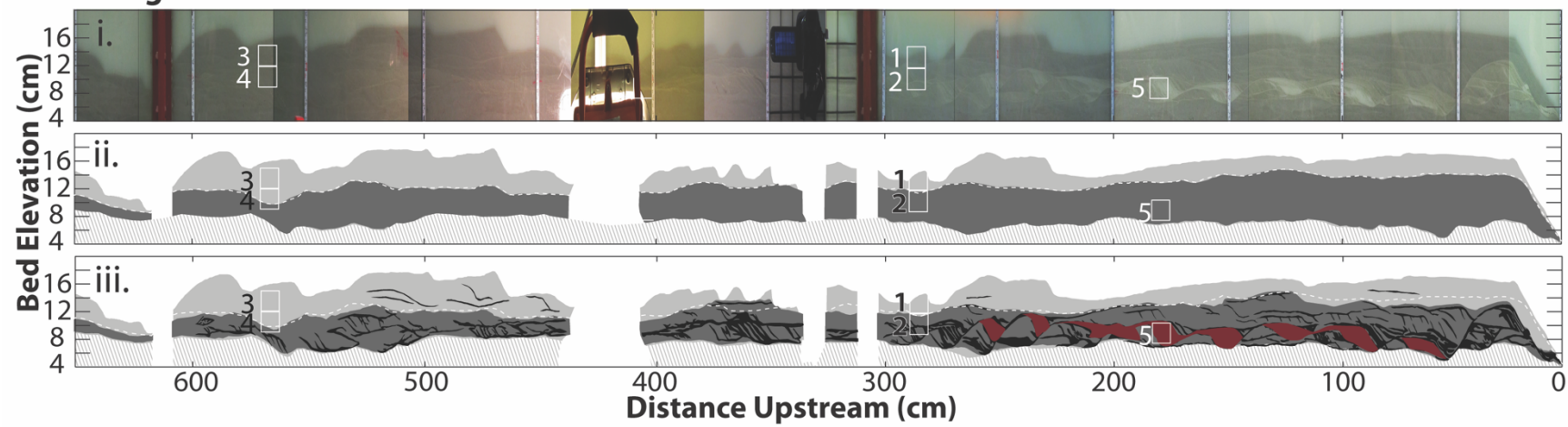
Bed Deposit Mapping Description and Images

Clay accumulations and bed areas are mapped on the vertically exaggerated images. Overlain topographic profiles and bed elevation points taken during the run helped determine which sediment was deposited during the bypass vs. aggradation phase. Clay accumulations were mapped on photographs of the bed. Clay accumulations appear whiter than the background sand, which is a tan color. Lighter colored sand indicates a higher abundance of intercalated clay (verified with weight percent results of individual samples from these regions). Long and thin accumulations of clay were mapped as drapes and larger, thicker deposits were mapped as clay lenses. Bed areas of each type of clay accumulation were quantified using image analysis tools in Matlab.

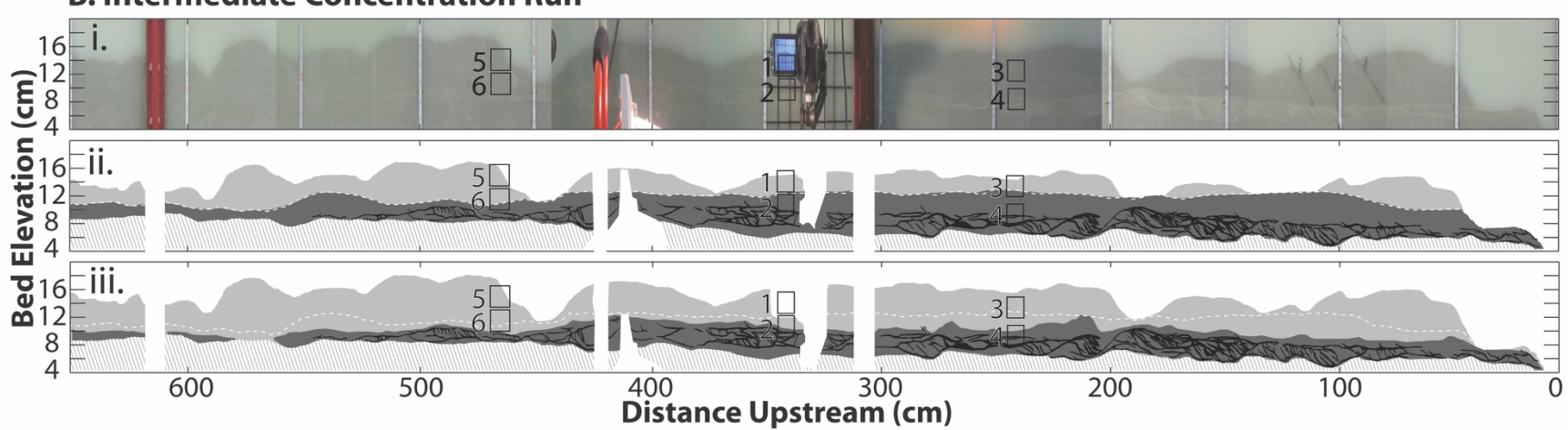
Figure DR12: Photographs and mapped clay accumulations of each run as seen through the glass wall of the flume.

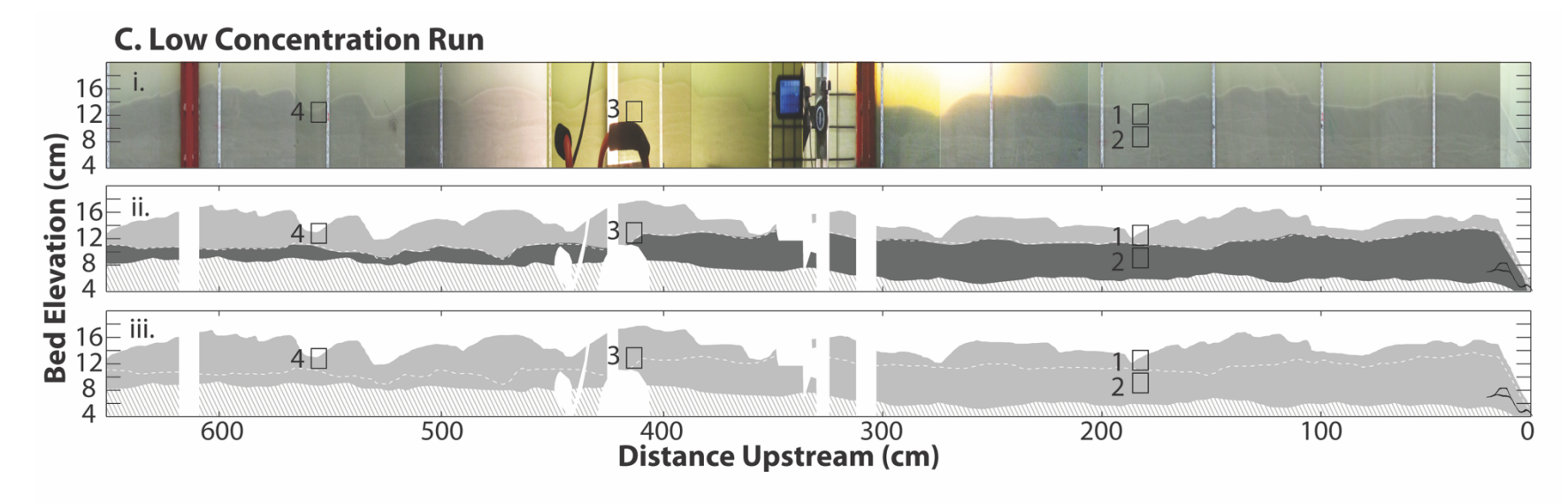
(Next pages) Vertical exaggeration is 3x. The y-axis is depth in centimeters. Hatched area is prerun sediment. White areas are obstructed views of the bed. The depth and downstream locations of samples (collected from the center of the flume, not along the flume walls) are noted by black boxes. Each experiment (A-D) includes the following: i) composite photograph of test section through glass panel, ii) map of clay accumulations preserved in the bed (black) and definition of aggradational phase area (dark gray) and bypass phase area (light gray), and iii) map of different types of clay accumulations observable in the bed including, intercalated clay (dark gray), clay drapes (black), and clay rich lenses (red).

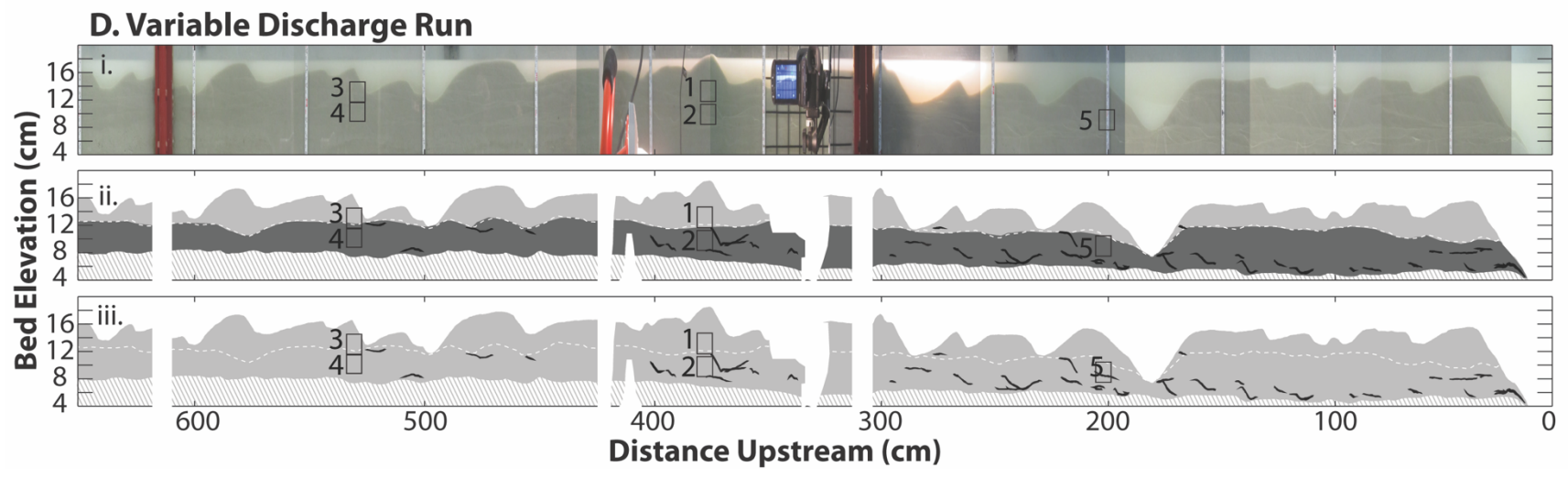




B. Intermediate Concentration Run







REFERENCES

- Baas, J.H., Best, J.L., and Peakall, J., 2011, Depositional processes, bedform development and hybrid bed formation in rapidly decelerated cohesive (mud-sand) sediment flows: Bedforms in decelerated cohesive flows: Sedimentology, v. 58, p. 1953–1987, doi:10.1111/j.1365-3091.2011.01247.x.
- Baas, J.H., Best, J.L., Peakall, J., and Wang, M., 2009, A Phase Diagram for Turbulent, Transitional, and Laminar Clay Suspension Flows: Journal of Sedimentary Research, v. 79, p. 162–183, doi:10.2110/jsr.2009.025.
- Beard, D.C., and Weyl, P.K., 1973, Influence of Texture on Porosity and Permeability of Unconsolidated Sand: AAPG Bulletin, v. 57, doi:10.1306/819A4272-16C5-11D7-8645000102C1865D.
- Bridge, J., and Demicco, R., 2008, Earth Surface Processes, Landforms and Sediment Deposits: Cambridge, Cambridge University Press, doi:10.1017/CBO9780511805516.
- Lamb, M.P., de Leeuw, J., Fischer, W.W., Moodie, A.J., Venditti, J.G., Nittrouer, J.A., Haught, D., and Parker, G., 2020, Mud in rivers transported as flocculated and suspended bed material: Nature Geoscience, v. 13, p. 566–570, doi:10.1038/s41561-020-0602-5.
- de Leeuw, J., Lamb, M.P., Parker, G., Moodie, A.J., Haught, D., Venditti, J.G., and Nittrouer, J.A., 2020, Entrainment and suspension of sand and gravel: Earth Surface Dynamics, v. 8, p. 485–504, doi:10.5194/esurf-8-485-2020.
- Packman, A.I., and MacKay, J.S., 2003, Interplay of stream-subsurface exchange, clay particle deposition, and streambed evolution: Water Resources Research, v. 39, doi:10.1029/2002WR001432.
- Sutherland, B.R., Barrett, K.J., and Gingras, M.K., 2015, Clay settling in fresh and salt water: Environmental Fluid Mechanics, v. 15, p. 147–160, doi:10.1007/s10652-014-9365-0.
- Wilkerson, G.V., and Parker, G., 2011, Physical Basis for Quasi-Universal Relationships Describing Bankfull Hydraulic Geometry of Sand-Bed Rivers: Journal of Hydraulic Engineering, v. 137, p. 739–753, doi:10.1061/(ASCE)HY.1943-7900.0000352.